Metal–Metal Bonds between Group 12 Metals and Tin: Structural Characterization of the Complete Series of Sn-M-Sn (M = Zn, Cd, Hg) Heterodimetallic Complexes

Matthias Lutz,[b] Bernd Findeis,[a] Matti Haukka,[b] Roland Graff,[a] Tapani A. Pakkanen,*[b] and Lutz H. Gade*[a]

Abstract: Reaction of the lithium triamidostannate [MeSi{$SiMe_2N(p\text{-Tol})$}$_3$-SnLi(OEt_2)] (**1**) with 0.5 molar equivalents of MCl_2 (M = Zn, Cd, Hg) in toluene afforded the corresponding heterodimetallic complexes [MeSi{$SiMe_2N(p\text{-Tol})$}$_3$Sn]$_2$M {M = Hg (**2**), Cd (**3**), and Zn (**4**)}. The molecular structures of the mercury and cadmium complexes were determined by X-ray diffraction and found to adopt a linear Sn-M-Sn metal—metal bonded array (d(Sn–Hg) 2.6495(2), d(Sn–Cd) 2.6758(1) Å), these being the first Hg–Sn and Cd–Sn bonds to be characterized by X-ray diffraction. That the Hg–Sn bonds are shorter than the Cd–Sn bonds in the isomorphous complexes is attributed to relativistic effects in the mercury system. In contrast, the structure of the Zn analogue is unsymmetrical with one stannate unit being Sn–Zn bonded (d(Sn(1)–Zn) 2.5782(4) Å), while the Zn^{II} atom bridges two amido functions of the second stannate cage, thus representing a second isomeric form of these complexes. The different degree of metal–metal bond polarity is reflected in the ^{119}Sn NMR chemical shifts of the three complexes. Variable-temperature NMR studies and a series of ^{1}H ROESY experiments of the cadmium complex **3** in solution revealed a dynamic exchange between the two isomers.

Keywords: cadmium · mercury · metal-metal bonds · N ligands · tin · zinc

Introduction

Metal–metal bond polarity[1] is normally linked to the difference of the coordination spheres of the bound metal atoms or to their different *horizontal* or *vertical* positions in the periodic table. In Group 12 of the periodic table there is an ideal combination of a significant variation of the properties of metal dications, the stability of a given oxidation state, and the accessibility of suitable starting materials. At the same time the extremes of transition-metal properties are covered, ranging from the typical first-row coordination behavior of divalent zinc to the structural chemistry of mercury(II), which is strongly influenced by the relativistic contraction of the 6s orbital and the destabilization of the 5d orbitals. This goes along with an increase of the covalency of ligand–metal and metal–metal bonding upon going down the group within Group 12.

Although Group 12 silyl compounds of the type $M(SiR_3)_2$ (M = Zn, Cd, Hg) have been studied systematically since the 1960s,[2, 3] much less is known about the heavier congeners in particular of heterodimetallic complexes between an element from Group 12 and tin. While there has been a small number of stable Ge–Hg[4] and Sn–Hg[5, 6] compounds reported, the corresponding Zn and Cd representatives remain extremely rare.[7, 8] A systematic study of tin–Group 12 heterodimetallic complexes, especially of their structural patterns is often thwarted by their pronounced light sensitivity and rapid degeneration at room temperature and their occurrence mainly as oily reaction products.

In previous studies we have shown that our tripodal triamidostannates(II), which act as anionic Sn^{II} nucleophiles, are suitable for the generation of a series of stable tin heterodimetallic complexes and resist oxidation by numerous salts of transition metals.[9, 10] They were therefore thought to be suitable building blocks for a systematic structural investigation of Sn–M bonded compounds in solution and in the crystalline state. Herein we provide the first Sn–Cd and Sn–Hg bonded complexes which have been structurally characterized by X-ray diffraction, along with only the second fully

[a] Prof. L. H. Gade, B. Findeis, R. Graff
Laboratoire de Chimie Organométallique et de Catalyse (UMR 7513)
Institut Le Bel, Université Louis Pasteur,
4, rue Blaise Pascal, 67070 Strasbourg (France)
Fax: (+33) 390-241531.
E-mail: gade@chimie.u-strasbg.fr

[b] Prof. T. A. Pakkanen, M. Lutz, M. Haukka
Department of Chemistry, University of Joensuu,
80101 Joensuu (Finland)
Fax: (+358)-13-2513344
E-mail: tapani.pakkanen@joensuu.fi

  0947-6539/02/0814-3269 $ 20.00+.50/0

structurally characterized Zn–Sn complex. This is supplemented by a comparative study of their different dynamic behavior in solution which is a result of the variation in the chemical properties of the three Group 12 metals.

Results and Discussion

Synthesis of the Sn-M-Sn heterodimetallic complexes (M = Zn, Cd, Hg) and their structural characterization by X-ray diffraction

Reaction of the lithium triamidostannate [MeSi{SiMe$_2$N(*p*-Tol)}$_3$SnLi(OEt$_2$)][9] (**1**) with 0.5 molar equivlants of MCl$_2$ (M = Zn, Cd, Hg) in toluene afforded the corresponding heterodimetallic complexes [MeSi{SiMe$_2$N(*p*-Tol)}$_3$Sn]$_2$M {M = Hg (**2**), Cd (**3**), and Zn (**4**)} as colorless to pale yellow microcrystalline solids for which the analytical data are consistent with the formulation given in Scheme 1.

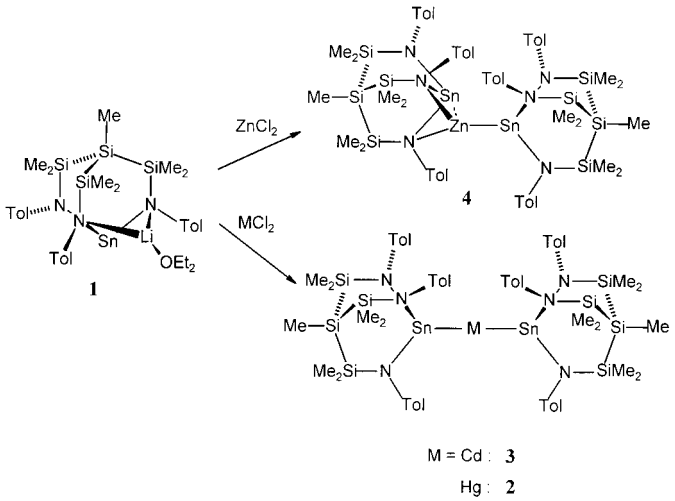

Scheme 1. Syntheses of complexes **2**–**4**.

The solid complexes **2** and **3** were found to be fairly airstable, but solutions of **2** decomposed slowly with concomitant formation of metallic mercury and an unidentified tin species upon prolonged exposure to light. Single crystals of all three complexes suitable for X-ray diffraction studies were obtained. The triclinic crystals of complexes **2** and **3** were found to be isomorphous. The molecular structure of compound **2** in the crystal, which is analogous to that of **3**, is displayed in Figure 1 along with the principal bond lengths and angles for both complexes. The compounds adopt the expected molecular structure containing a linear Sn-M-Sn unit, with the central Hg or Cd atom lying on a crystallographic inversion center. The two MeSi{SiMe$_2$N(*p*-Tol)}$_3$Sn units are therefore bonded in an exactly linear fashion to the mercury center (Sn(1)-Hg-Sn(1′) 180.00°) and are staggered with respect to each other (D_{3d} symmetry). The Sn–Hg bond length (d(Sn–Hg) 2.6492(2) Å), which is the first to be determined by X-ray crystallography, is shorter than the sum of the covalent radii ($r_{Sn} + r_{Hg} = 2.90$ Å),[11] but is significantly longer than the X–Hg (X = Si, Ge) distances

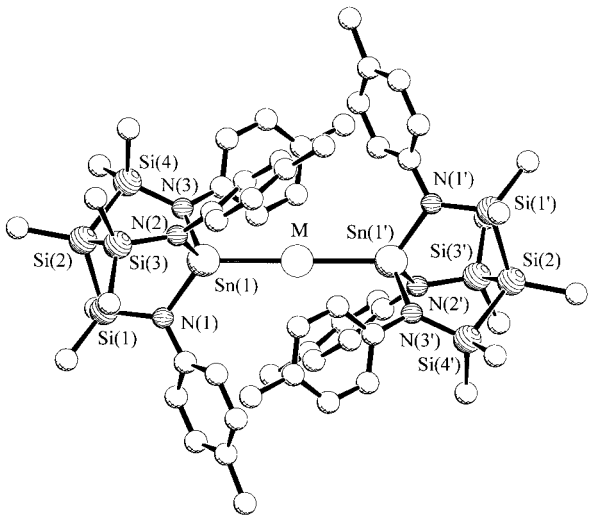

Figure 1. Molecular structure of **2** and **3** in the crystal. Selected bond lengths [Å] and interbond angles [°]; (M = Hg) **2**: Sn(1)–Hg 2.6495(2), N(1)–Sn(1) 2.054(2), N(2)–Sn(1) 2.075(3), N(3)–Sn(1) 2.074(2); Sn(1)-Hg-Sn(1′) 180.00, N(1)-Sn(1)-N(3) 105.39(10), N(1)-Sn(1)-N(2) 106.51(10), N(3)-Sn(1)-N(2) 102.18(10), N(1)-Sn(1)-Hg 124.54(7), N(3)-Sn(1)-Hg 110.04(7), N(2)-Sn(1)-Hg 105.99(7); (M = Cd) **3**: Sn(1)–Cd 2.6758(2), N(1)–Sn(1) 2.0578(18), N(2)–Sn(1) 2.0823(19), N(3)–Sn(1) 2.0882(18), Sn(1)-Cd-Sn(1′) 180.00, N(1)-Sn(1)-N(3) 105.53(7), N(1)-Sn(1)-N(2) 105.85(7), N(3)-Sn(1)-N(2) 100.71(7), N(1)-Sn(1)-Cd 128.30(5), N(3)-Sn(1)-Cd 107.92(5), N(2)-Sn(1)-Cd 105.27(5).

found in the known mercury complexes with the lighter Group 14 elements, such as [{(C$_6$F$_5$)$_3$Ge}$_2$Hg] (2.483 Å),[4a] [{(Me$_3$SiSi(Me$_2$))$_3$Si}$_2$Hg$_2$] (2.485 Å),[12a] [{Ph$_3$Si}$_2$Hg] (2.494 Å),[12b] [{(Me$_3$Si)$_3$Ge}$_2$Hg] (2.512 Å),[4b] and [{Ph$_3$Ge}$_2$Hg] (2.543 Å).[4c] There are relatively short contacts between the Hg atom and the arene rings of the tolyl units in the ligands (for instance C(19)–Hg(1) 3.227, C(23)–Hg(1) 3.582, centroid(C(13)–C(19))–Hg(1) 3.361, centroid(C(22)–C(23))–Hg(1) 3.477 Å); however, these seem to be imposed by the orientation of the ligand periphery of the tripodal amides rather than being significant in their own right. The corresponding arene–Cd distances are, accordingly, very similar.

The Sn–Cd bond length in the isostructural complex **3** was found to be 2.6758(1) Å which is significantly longer than the Hg–Sn distance discussed above. Here again, there is no precedent in the literature as far as metal–metal bonding between these elements is concerned, however, it is notable that the lighter element appears to possess the greater ionic radius. Such an inversion of the atom/ion sizes is quite common in the chemistry of the early transition elements which follow the lanthanoid block (e.g. Zr/Hf) and in the latter case a consequence of the lanthanoid contraction.[13] For the late transition metals the relativistic contraction of 6s valence shell in the third-row elements becomes an increasingly important factor. Schmidbaur and co-workers have found such an inverse relation for isostructural gold(I) and silver(I) complexes and it is to be assumed that the case at hand is analogous.[14]

In both complexes the peripheral tolyl groups adopt mutual edge-to-face orientations so that a total of six π–π interactions (ring centroid—ring centroid 3.839–4.156 Å) encapsulate the metal core of the complex. This arrangement is

  0947-6539/02/0814-3270 $ 20.00+.50/0 *Chem. Eur. J.* **2002**, *8*, No. 14

reminiscent of the centrosymmetric sextuple phenyl embraces identified by Dance and co-workers as a supramolecular motif in $\{Ph_4P^+\}_2$ complexes[15] and may contribute to the stability of the dinuclear compounds.

In contrast to the isomorphous compounds **2** and **3**, the X-ray diffraction study of the Sn-Zn-Sn heterodinuclear complex $[MeSi\{SiMe_2N(p\text{-}Tol)\}_3Sn]_2M$ (**4**) established a significantly different molecular structure which is depicted in Figure 2 along with the principal metric parameters.

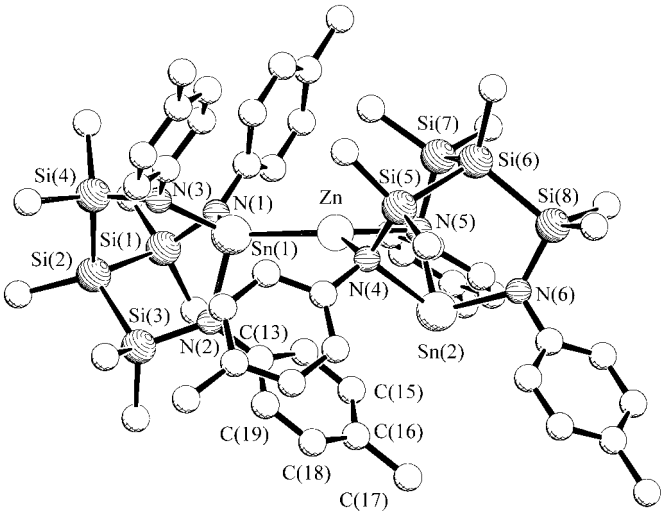

Figure 2. Molecular structure of **4** in the crystal. Selected bond lengths [Å] and interbond angles [°]: Zn–Sn(1) 2.5782(4), Zn–Sn(2) 2.9930(4), N(1)–Sn(1) 2.086(2), N(2)–Sn(1) 2.069(2), N(3)–Sn(1) 2.071(2), N(4)–Sn(2) 2.357(2), N(5)–Sn(2) 2.337(2), N(6)–Sn(2) 2.123(2), N(4)–Zn 2.044(2), N(5)–Zn 2.035(2); N(2)-Sn(1)-N(3) 101.60(9), N(2)-Sn(1)-N(1) 100.48(9), N(3)-Sn(1)-N(1) 102.08(9), N(2)-Sn(1)-Zn 104.07(7), N(3)-Sn(1)-Zn 123.70(6), N(1)-Sn(1)-Zn 120.89(6), N(6)-Sn(2)-N(5) 101.75(9), N(6)-Sn(2)-N(4) 104.67(9), N(5)-Sn(2)-N(4) 76.04(8), N(6)-Sn(2)-Zn 128.21(7), N(4)-Sn(2)-Zn 42.90(5), N(5)-Sn(2)-Zn 42.71(6), Sn(1)-Zn-Sn(2) 140.385(13), N(5)-Zn-N(4) 90.29(9), N(4)-Zn-Sn(1) 131.46(7), N(5)-Zn-Sn(1) 135.92(6), N(4)-Zn-Sn(2) 51.73(6), N(5)-Zn-Sn(2) 51.18(7).

In the crystal, complex **4** comprises two geometrically inequivalent $\{MeSi\{SiMe_2N(p\text{-}Tol)\}_3Sn\}$ metal–ligand units. The tin atom in one of these metallacages is directly bonded to the zinc atom to form an unsupported Zn–Sn bond with a bond length of d(Sn(1)–Zn) 2.5782(4) Å. A comparable value for a direct Sn–Zn bond has been recently reported for zinc [bis{3-(dimethylamino)propyl-*C*,*N*}tin]bis(dibenzoylmethanato)(Sn–Zn) (d(Sn–Zn) 2.634(6) Å).[16] In contrast, the tripodal amido ligand in the second stannate unit acts a bridging ligand, binding both the tin and zinc atoms. As a consequence of simultaneous tin and zinc bonding and of the electron-deficient nature of the zinc atom, the Sn–N bond lengths in the C_S symmetrical subunit differ considerably from each other (d(N(4)–Sn(2)) 2.357(2), d(N(5)–Sn(2)) 2.337(2), d(N(6)–Sn(2)) 2.123(2) Å). This is to be compared to the C_{3v} symmetrical subunit for which almost equal Sn–N bond lengths were found (d(N(1)–Sn(1)) 2.086(2), d(N(2)–Sn(1)) 2.069(2), d(N(3)–Sn(1)) 2.071(2) Å). The latter are also considerably shorter which we believe to be a consequence of the coordination of a Lewis acidic metal center to the tin atom. The shortening of the Sn–N bonds in complexes between Sn and transition metals containing this triamidostannate cage in comparison to the lithium stannate(II) has been previously observed. In compound **4** the N–Zn-bonded stannate unit therefore visibly retains its anionic stannate character and the complex may be formally described as a zwitterionic species.

As a result of intramolecular Zn–N coordination (d(N(4)–Zn) 2.044(2), d(N(5)–Zn) 2.035(2) Å) the zinc atom in **4** is tricoordinate with an additional contact to the second tin atom (d(Zn–Sn(2)) 2.9930(4) Å). The degree of Sn–Zn bonding across the bridging amido ligand is difficult to assess but thought to be rather weak.

Owing to the reduced symmetry and the tilting of the Sn(2) cage with respect to the Sn(1)–Zn axis, the arrangement of its ligand tolyl groups is also much less symmetrical. In fact, as is evident in the view of the molecule chosen in Figure 2, one of the tolyl groups of the Sn(1) triamidotin cage (C(13)–C(19)) is now almost embedded between two of the tolyl groups of the Sn(2) unit. This places it exactly within the high shift anisotropy cones of two Sn(2) tolyl fragments, a situation which is expected to give rise to unusual chemical shifts of the ^{1}H NMR resonances of this tolyl group if intramolecular Sn–Zn rotation is frozen out in the low-temperature limit (vide infra).

The structures and dynamic behavior of the Sn-M-Sn complexes 2–4 in solution

For the Sn-Hg-Sn complex **2** the ^{1}H, ^{13}C, and ^{29}Si NMR spectroscopic patterns in the spectra recorded at 291 K are consistent with a threefold symmetry in solution. The chemical shift of the ^{119}Sn NMR resonance of **2** ($\delta =$ 266.2 ppm) is significantly shifted to lower field compared to the ^{119}Sn NMR signal of the stannate **1** ($\delta = -96.3$ ppm), and the ^{199}Hg NMR signal is observed at $\delta = -267.8$ ppm (ext. standard: $HgMe_2$). We were unable to observe $^{117/119}$Sn–^{199}Hg coupling in solution which is probably due to the rapid relaxation of the Sn nuclei caused by the quadrupolar ^{14}N environment.

The ^{1}H, ^{13}C, ^{29}Si, and ^{119}Sn NMR spectra of the Sn-Zn-Sn heterodimetallic complex **4**, recorded at 291 K, reflect the reduced symmetry of the system in comparison to its mercury analogue. The analysis of the signal pattern due to the Si-bonded methyl groups is particularly instructive (Figure 3a). The intense, slighly broadened resonance at $\delta = 0.57$ ppm is attributed to the $Si(CH_3)_2$ groups and the singlet at $\delta =$ 0.26 ppm to the apical $SiCH_3$ group of the Sn–Zn-bound stannate cage. Rotation around the Sn–Zn is apparently still a rapid process at this temperature and generates the effective local threefold symmetry although the visible resonance broadening indicates a significant activation barrier. In the second stannate fragment in which the Zn ion bridges the two amido functions the local symmetry is reduced to mirror symmetry which gives rise to three proton signals for the $Si(CH_3)_2$ units ($\delta = 0.02$, 0.06, 0.32 ppm) and the resonance of the second "apical" Si-CH_3 group ($\delta = -0.01$ ppm). The signals of the peripheral tolyl groups lie in the typical range around $\delta = 2.2$ ($CH_3C_6H_4$) and 6.7–7.5 ppm (aromatic protons). However, at 291 K and below a resonance set of a single

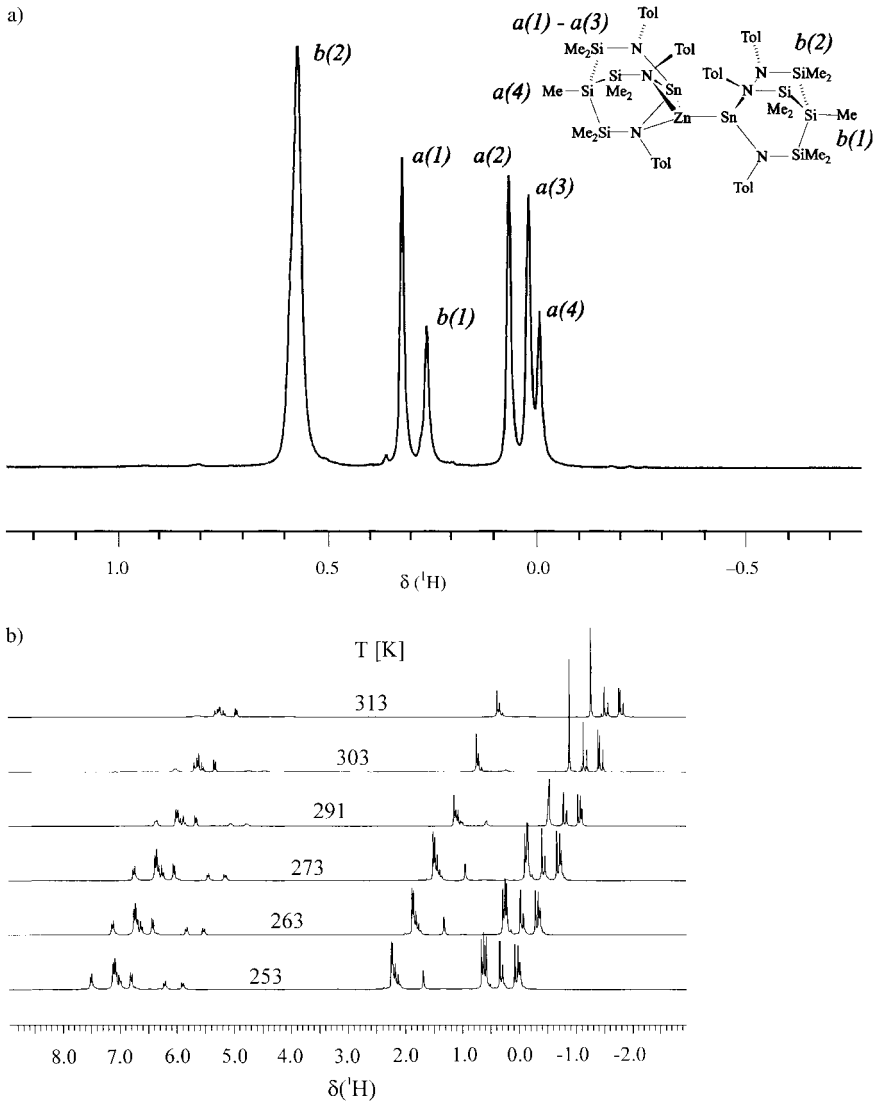

Figure 3. a) $Si(CH_3)_2$ and $SiCH_3$ resonances in the ^1H NMR spectrum of **4** recorded at 291 K. b) Variable-temperature ^1H NMR series of complex **4**.

tolyl group at unusually high field emerges ($\delta = 1.67$ ($CH_3C_6H_4$) and 5.87, 6.15 ppm (AB system of the aromatic protons)). We attribute this set of signals to the unique tolyl group of the Sn(1) fragment in the molecular structure depicted in Figure 2. The principal changes upon lowering the temperature to 253 K is the sharpening up of this high field tolyl resonances due to the freezing out the intramolecular Sn–Zn rotation (Figure 3b). This goes along with the splitting of the $Si(CH_3)_2$ signal at $\delta = 0.57$ ppm into three singlets ($\delta =$ 0.58, 0.62, and 0.65 ppm).

This correspondence of the NMR signal pattern with the molecular structure of **4** found in the solid state is supported by the observation of five ^{29}Si NMR resonances at $\delta = -98.2$, -88.2 ($2 \times$ SiMe), -6.1, 0.5, and 6.0 ppm ($3 \times SiMe_2$), and two ^{119}Sn NMR resonances ($\delta = -153.5$ and -91.2 ppm). The chemical shift of the ^{119}Sn NMR resonances strongly depends on the symmetry around the tin nucleus and therefore changes to lower frequencies upon going from a tetrahedral to a trigonal-monopyramidal coordination geometry.[17] Consequently the signal at $\delta = -91.2$ ppm is attributed to the tin nucleus possessing a direct Sn–Zn bond, while the resonance at higher field shift ($\delta = -153.5$ ppm) is due to the stannate-type tin nucleus Sn(2).

Whereas the NMR spectra of complexes **2** and **4** are consistent with the molecular structures of both compounds determined in the X-ray diffraction experiment, the ^1H NMR spectrum of the Sn-Cd-Sn complex **3** recorded in [D_8]toluene at 291 K proved to be more complicated. The presence of two isomers of complex **3**, a symmetrical form **3a** as found in its crystal structure, and a nonsymmetrical form **3b** analogous to the structure found for **4** in the crystal structure analysis can be readily inferred from the signal pattern of the Si-bonded methyl groups observed at this temperature as well as the detection of two ^{113}Cd NMR resonances ($\delta = 310$, 201 ppm; external reference: $Cd(ClO_4)_2/H_2O$, 1.0 M).

In the methylsilyl chemical shift range of the ^1H NMR spectrum depicted in Figure 4a there are eight methyl resonances in total, of which the signal at $\delta = 0.17$ ppm is attributed to the apical Si-CH_3 group and the singlet at $\delta = 0.52$ ppm to the three $Si(CH_3)_2$ units in each of the two aminostannate cages of the symmetrical, linear Sn-Cd-Sn complex **3a**. For the second isomer, **3b**, the Sn–Cd bonded stannate cage appears to undergo rapid internal rotation around the Sn–Cd axis, generating local threefold symmetry which is reflected in the two signal pattern of the Si-CH_3 ($\delta =$ 0.26 ppm) and the $Si(CH_3)_2$ ($\delta = 0.59$ ppm) units. In the second stannate fragment the local symmetry is reduced to mirror symmetry due to the bridging of two of the amido N atoms by the cadmium ion. This leads to three resonances for the $Si(CH_3)_2$ groups ($\delta = 0.00$, 0.12, 0.36 ppm) and the signal for the apical methyl group at $\delta = 0.02$ ppm.

The spectrum shown in Figure 4a represents an intermediate dynamic regime in the equilibrium between the two isomeric forms **3a** and **3b**. At 253 K the $SiMe_2$ resonance signal of the Sn–Cd bonded stannate unit in **3b** is split indicating a hindered rotation around the Sn–Cd bond (Figure 4b). As in the low-temperature ^1H NMR spectrum of the zinc analogue **4**, the set of proton signals of one of the tolyl groups is observed at remarkably high field which we attribute to the same structural environment as discussed in detail above. Upon raising the sample temperature to 373 K in

  0947-6539/02/0814-3272 $ 20.00+.50/0 *Chem. Eur. J.* **2002**, *8*, No. 14

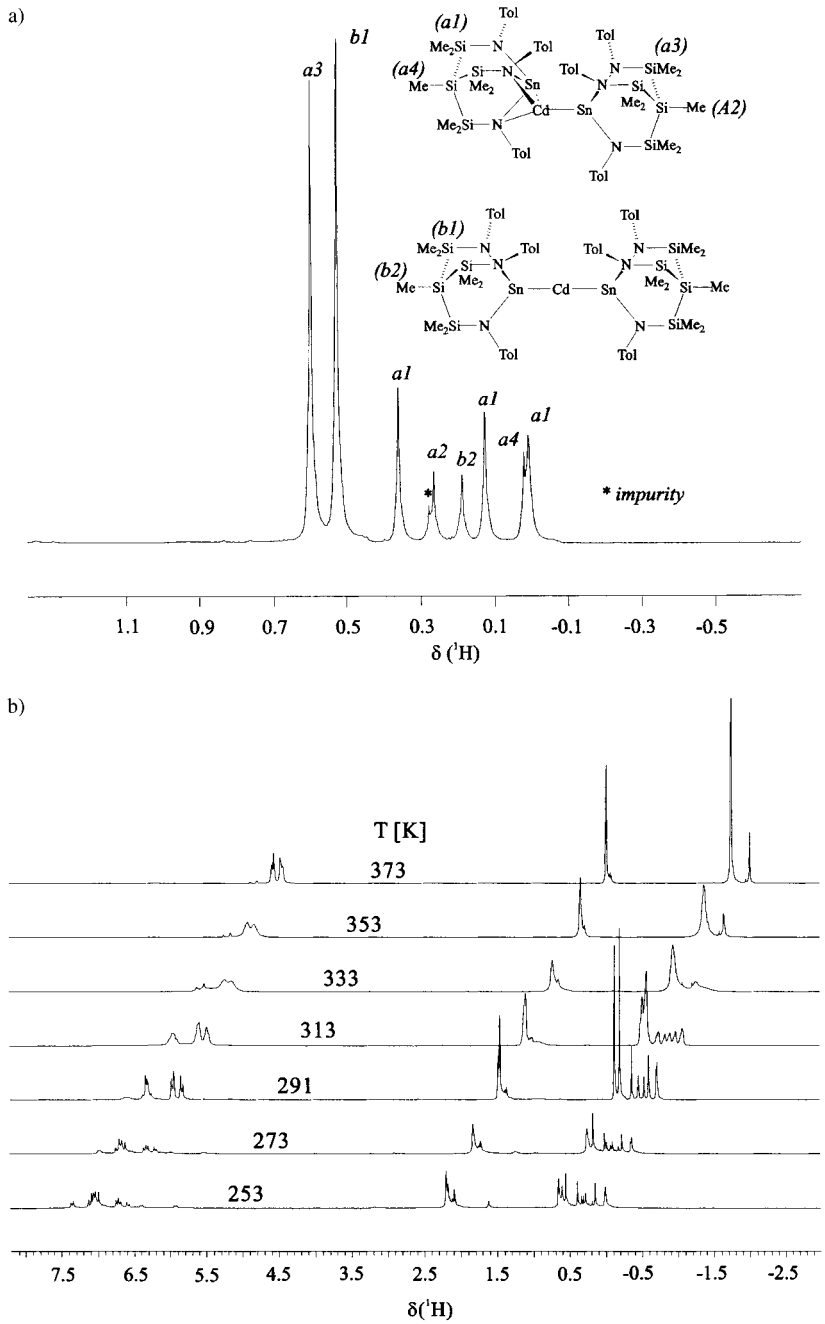

Figure 4. a) $Si(CH_3)_2$ and $SiCH_3$ resonances in the ^1H NMR spectrum of **3** recorded at 291 K. b) Variable-temperature ^1H NMR series of complex **3**.

a variable-temperature series of ^1H NMR spectra all resonances coalesce and a high-temperature limit is attained which has the same spectral pattern as observed for the static Sn-Hg-Sn complex **2** (Figure 4b). This indicates that at 373 K the exchange between the two isomers **3a** and **3b** as well as the intramolecular exchange of the different μ_2-bridging Cd-amide positions in **3b** is rapid on the NMR time scale (Scheme 2).

The exchange networks for the $Si(CH_3)_2$ protons and the resonances of the apical $SiCH_3$ groups in **3** were also studied by ^1H-ROESY spectroscopy. The variant of this method used in this study was developed by Desvaux and Goldman to suppress the TOCSY type contributions as well as the COSY cross peaks.[18a] The methyl ^1H NMR chemical shift region is represented in Figure 5 and is consistent with the conclusions drawn from the variable-temperature study.

A comparison of the properties and the behavior of the Group 12 metals in the Sn–M bonded complexes 2–4

The use of identical building blocks in compounds **2**–**4** allows a meaningful comparison of these metal–metal bonds. The metal–metal bonds in the Sn-Hg-Sn complex **2** is polar but primarily covalent, as is evident from the strong deshielding of the ^{119}Sn nuclei ($\delta = 266.2$ ppm) compared to the the lithium stannate(II) "ligand" ($\delta = -96.3$). The linear arrangement is reinforced by the relativistic contraction of the valence 6s shell as is observed in most mercury compounds.

For the zinc complex, on the other hand, the chemical shifts of the two ^{119}Sn NMR resonances are at high field ($\delta = -92.8$, -155.0 ppm) which indicates the retention of the stannte(II) character of the tin fragment. Metal–metal bonding in this case is thus strongly ionic and the Sn−Zn bond is to be seen as a "classical metal–ligand" coordinative bond. This and the preference of zinc(II) for higher coordination numbers explain the nonsymmetrical molecular structure for **4** both in solution and in the solid state. The amido-N coordination of the zinc(II) center offers a better match of chemical hardness/softness of the donor–acceptor interaction,[19] and it is assumed that this would be the preferred coordination mode for both stannate units (rendering the zinc tetracoordinate), if the steric interactions of the peripheral tolyl groups were not in the way of such an arrangement. Finally, the cadmium–tin complex **3** represents a heterodimetallic species with an intermediate bond polarity between those in **2** and **4**, as is evident from the ^{119}Sn NMR chemical shifts found for this species. In the nonsymmetrical isomer **3b**, the ^{119}Sn nucleus of the amido-N coordinated stannate fragment resonates at $\delta = -142.7$ ppm which is very similar to the equivalent Sn environment in the Zn–Sn compound. However, the signal of the cadmium-bonded tin nucleus in **3** is observed

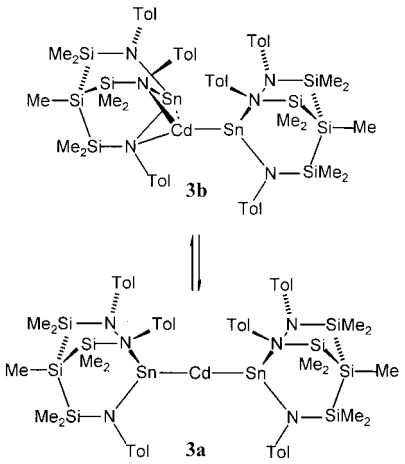

Scheme 2. Dynamic interconversion of the isomers **3a** and **3b**.

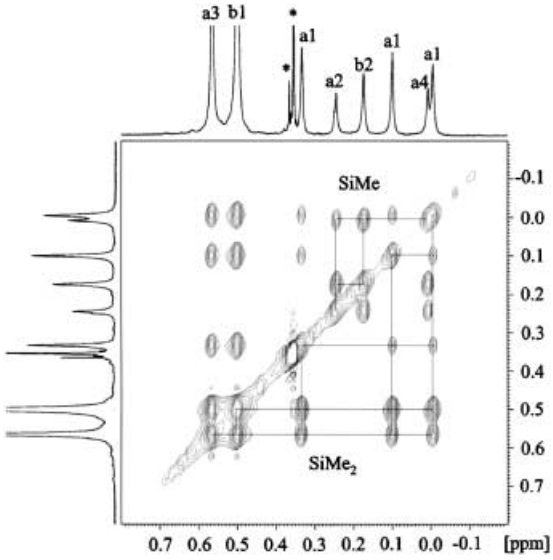

Figure 5. ^{1}H ROESY spectrum recorded at 313 K (t_{mix} = 300 ms): The exchange networks for the $Si(CH_3)_2$ protons and the resonances of the apical $SiCH_3$ groups in **3** are indicated; * = impurity.

at $\delta = -22.2$ and thus at considerably lower field than in **4**. The position of **3** between the two extremes **2** and **4** is additionally manifested in the dynamic behaviour observed in solution in which the two isomeric forms exchange rapidly.

Conclusion

This study has provided a detailed structural investigation of tin – Group 12 heterodimetallic complexes and with it the first structurally characterized Sn–Cd and Sn–Hg bonds. As in our previous work, the use of the tripodal triamidostannate cage as a building block for heterodimetallic complexes has proved not only to yield stable crystalline compounds but allowed the investigation of a remarkable, decomposition-free dynamic behavior in solution. This study now provides the basis for a detailed theoretical analysis of the variation of metal-metal bonding in such compounds. Our current and future work also aims at extending this approach to heterometallic arrays containing oligomercury units bound to the stannates.

Experimental Section

All reactions were performed in flame-dried glassware under an inert gas atmosphere of dry nitrogen (desiccant P_4O_{10}, Granusic, J.T. Baker) using standard Schlenk techniques, or in a glovebox. Toluene, *n*-pentane, [D_6]benzene, [D_8]toluene, and [D_8]tetrahydrofuran were distilled prior to use from sodium potassium alloy and stored under nitrogen in resealable bulbs. Solids were separated from suspensions by filtration through dried Celite.

The ^{1}H, ^{13}C, and ^{119}Sn NMR spectra were recorded on a Bruker Avance 250 and a Bruker AMX 400 FT NMR spectrometer, respectively. The ^{29}Si and ^{199}Hg NMR spectra were recorded on Bruker Avance 250 FT NMR and AMX 400 spectrometers. ^{1}H and ^{13}C NMR data are listed in parts per million (ppm) relative to tetramethylsilane and were referenced by using the residual protonated solvent peak (^{1}H) or the carbon resonance (^{13}C). ^{29}Si, ^{119}Sn, ^{113}Cd, and ^{199}Hg NMR data are listed in ppm relative to the external standards tetramethylsilane, tetramethyltin, $Cd(ClO_4)_2/H_2O$ (1.0 M) and $HgMe_2$, respectively.

In the ^{1}H ROESY experiment[18] mixing times were varied between 50 and 300 ms (in increments of 50 ms). The spin lock field had a spectral coverage of 5000 Hz and the off resonance carrier was set at an offset at $tg\theta = \gamma B_1/\omega \approx 54°$. Relaxation delay: 3 s; TD: 2 K, 512 increments. The spectra were processed after zero filling in both dimensions to 2 K × 2 K and after cos^2-apodization in both dimensions.

Elemental analyses were carried out with a Leco CHNS-932 microanalyzer and a CE-instruments EA 1110 CHNS-O microanalyzer. The lithium triamidostannate [$MeSi\{SiMe_2N(p\text{-}Tol)\}_3SnLi(OEt_2)$] (**1**)[9] was prepared according to a literature procedure. The commercially available metal halides $CdCl_2$, and $ZnCl_2$ were dehydrated by means of refluxing in $SOCl_2$ for 24 h prior to use and subsequently thoroughly dried in vacuum.

General procedure for the preparation of Tin – Group 12 heterobimetallic compounds

Precooled toluene (15 mL) was added to a solid mixture of [$MeSi\{SiMe_2N(p\text{-}Tol)\}_3SnLi(OEt_2)$] (**1**) (733 mg, 1.00 mmol) and the dehydrated Group 12 metal dichloride (0.50 mmol; $ZnCl_2$: 68.2 mg, $CdCl_2$: 91.7 mg, $HgCl_2$: 136 mg, respectively) which was cooled to −78 °C. The reaction mixture was warmed up to ambient temperature within a period of 12 h and subsequently filtered through Celite. The residue was extracted with hot toluene (20 mL) and the resulting solution was concentrated to about 10 mL. Storage at −50 °C afforded the mixed tin heterobimetallic compound as a microcrystalline solid. The obtained residue was washed with *n*-pentane (5 mL) and dried in vacuum.

[$(MeSi\{SiMe_2N(p\text{-}Tol)\}_3Sn)_2Hg$] (2): yellow crystals, yield: 511 mg (68 %); ^{1}H NMR (250.13 MHz, [D_8]toluene, 295 K): $\delta = 0.16$ (s, 6H; $SiCH_3$), 0.52 (s, 36H; $Si(CH_3)_2$), 2.21 (s, 18H; $CH_3C_6H_4$), 6.52 (d, $^3J_{H,H} = 8.3$ Hz, 12H; $H^{2,6}$ of $CH_3C_6H_4$), 6.71 ppm (d, $^3J_{H,H} = 8.3$ Hz, 12H, $H^{3,5}$ of $CH_3C_6H_4$); {^{1}H}^{13}C NMR (62.90 MHz, [D_8]toluene, 295 K): $\delta = -15.1$ ($SiCH_3$), 3.4 ($Si(CH_3)_2$), 20.5 ($CH_3C_6H_4$), 124.1 ($C^{2,6}$), 129.9 (C^4), 130.6 ($C^{3,5}$), 149.5 ppm (C^1); {^{1}H}^{29}Si NMR (49.7 MHz, [D_8]THF, 295 K): $\delta = -89.8$ ($SiCH_3$), 2.4 ppm ($Si(CH_3)_2$); {^{1}H}^{119}Sn NMR (93.3 MHz, [D_8]THF, 295 K): $\delta =$ 266.2 ppm (Sn-Hg-Sn); {^{1}H}^{199}Hg NMR (44.79 MHz, [D_8]toluene, 295 K): $\delta = -267.8$ ppm (Sn-Hg-Sn); elemental analysis (%) calcd for $C_{56}H_{84}HgN_6Si_8Sn_2$ (M_r = 1503.98): C 44.72, H 5.63, N 5.59; found: C 45.09, H 5.46, N 5.72.

[$(MeSi\{SiMe_2N(p\text{-}Tol)\}_3Sn)_2Cd$] (3): Pale-yellow crystals, yield: 517 mg (73 %); ^{1}H NMR (250.13 MHz, [D_8]toluene, 373 K): $\delta = 0.16$ (s, 6H; $SiCH_3$), 0.42 (s, 36H; $Si(CH_3)_2$), 2.15 (s, 18H; $CH_3C_6H_4$), 6.62 (d, $^3J_{H,H} =$ 7.5 Hz, 12H; $H^{2,6}$ of $CH_3C_6H_4$), 6.74 ppm (d, $^3J_{H,H} = 7.5$ Hz, 12H; $H^{3,5}$ of $CH_3C_6H_4$); {^{1}H}^{13}C NMR (62.90 MHz, [D_8]toluene, 291 K): $\delta = -15.0$ ($SiCH_3$), −14.9 ($SiCH_3$), −14.5 ($SiCH_3$), 1.9 ($Si(CH_3)_2$), 3.4 ($Si(CH_3)_2$), 4.4 ($Si(CH_3)_2$), 6.2 ($Si(CH_3)_2$), 20.5 ($CH_3C_6H_4$), 20.7 ($CH_3C_6H_4$), 124.3, 127.1, 129.5, 129.8, 129.9, 130.3, 130.8, 131.8, 132.6, 146.4, 147.8, 150.8 ppm (aromatic tolyl-C); {^{1}H}^{13}C NMR (62.90 MHz, [D_8]toluene, 363 K): $\delta =$ −14.9 ($SiCH_3$), 3.8 (br, $SiCH_3$), 20.7 ($CH_3C_6H_4$), 125.7 (br), 130.9 ppm (aromatic carbons); {^{1}H}^{29}Si NMR (49.69 MHz, [D_8]toluene, 291 K): $\delta =$ −97.8 ($SiCH_3$), −88.9 ($SiCH_3$), −87.7 ($SiCH_3$), −7.2 ($Si(CH_3)_2$), −1.9 ($Si(CH_3)_2$), 1.1 ($Si(CH_3)_2$), 5.0 ($Si(CH_3)_2$); {^{1}H}^{119}Sn NMR (93.3 MHz, [D_8]toluene, 295 K): $\delta = -22.2$, −142.7; {^{1}H}^{113}Cd NMR ([D_8]toluene,

  0947-6539/02/0814-3274 $ 20.00+.50/0 *Chem. Eur. J.* **2002**, *8*, No. 14

295 K): 310, 201; elemental analysis calcd for $C_{56}H_{84}CdN_6Si_8Sn_2$ [1415.80]: C 47.51, H 5.98, N 5.94; found: C 47.64, H 6.07, N 5.88.

[(MeSi{SiMe$_2$N(*p*-Tol)}$_3$Sn)$_2$Zn] (4): Colorless crystals, yield: 403 mg (57%); ^{1}H NMR (250.13 MHz, [D$_8$]toluene, 323 K): $\delta = 0.00$ (s, 3H; $SiCH_3$), 0.02 (s, 6H; $Si(CH_3)_2$), 0.05 (s, 6H; $Si(CH_3)_2$), 0.24 (s, 3H; $SiCH_3$), 0.30 (s, 6H; $Si(CH_3)_2$), 0.53 (s, 18H; $Si(CH_3)_2$), 2.12 (s, 3H; $CH_3C_6H_4$), 2.16 (s, 6H; $CH_3C_6H_4$), 2.23 (s, 9H; $CH_3C_6H_4$), 6.71–7.09 ppm (m, 24H, $CH_3C_6H_4$); {^{1}H}^{13}C NMR (62.90 MHz, C_6D_6, 323 K): $\delta = -15.0$ ($SiCH_3$), -14.5 ($SiCH_3$), 2.2 ($Si(CH_3)_2$), 4.3 ($Si(CH_3)_2$), 5.3 ($Si(CH_3)_2$), 20.66 ($CH_3C_6H_4$), 20.68 ($CH_3C_6H_4$), 20.71 ($CH_3C_6H_4$), 117.3, 125.6, 127.2, 129.5, 129.9, 130.2, 130.6, 132.2, 133.2, 145.8, 147.2, 150.6 ppm (aromatic carbons); {^{1}H}^{29}Si NMR (49.69 MHz, [D$_8$]toluene, 291 K): $\delta = -98.2$ ($SiCH_3$), -88.2 ($SiCH_3$), -6.1 ($Si(CH_3)_2$), 0.5 ($Si(CH_3)_2$), 6.0 ($Si(CH_3)_2$); {^{1}H}^{119}Sn NMR (149.18 MHz, [D$_8$]toluene, 291 K): $\delta = -153.5$ (N_3-Sn), -91.2 (N_3-Sn-ZnN_2); elemental analysis calcd (%) for $C_{56}H_{84}N_6Si_8Sn_2Zn \cdot 0.5\,C_6H_5CH_3$ ($M_r = 1414.84$): C 50.51, H 6.27, N 5.94; found: C 50.55, H 6.41, N 5.91.

X-ray crystallographic study

The X-ray diffraction data were collected with a Nonius KappaCCD diffractometer using $Mo_{K\alpha}$ radiation ($\lambda = 0.71073$ Å) with a Collect data collection program.[20] The Denzo-Scalepack program package[21] was used for cell refinements and data reduction. The structures **2** and **4** were solved by direct methods by using the SIR97[22] with the WinGX[23] graphical user interface. Structure **3** was solved by the Patterson method by using the DIRDIF-99 program.[24] A multiscan absorption correction based on equivalent reflections (XPREP in SHELXTL version 6.12)[25] was applied to all data (T_{max}/T_{min} were 0.38729/0.25607, 0.33751/0.30057 and 0.38284/0.32612 for **2**, **3**, and **4** respectively). Structures were refined against F^2 using the SHELXL97 program.[26] All hydrogen atoms were placed in idealized positions and constrained to ride on their parent atom. The asymmetric unit of **4** contains half a molecule of toluene. The solvent molecule is disordered around the center of symmetry. Carbon atoms of the toluene molecule were refined isotropically with equal U_{iso} and with fixed carbon–carbon distances. The crystallographic data are summarized in Table 1.

CCDC-179103 (**2**), CCDC-179104 (**3**), and CCDC-179105 (**4**) contain the supplementary crystallographic data (excluding structure factors) for the structures reported in this paper. These data can be can be obtained free of charge via www.ccdc.cam.ac.uk/conts/retrieving.html (or from the Cambridge Crystallographic Data Centre, 12 Union Road, Cambridge CB2 1EZ, UK; fax: (+44) 1223-336033; or deposit@ccdc.cam.ac.uk).

Table 1. Crystal data and structure refinement for **2**, **3**, and **4**.

	2	**3**	**4**
molecular formula	$C_{56}H_{84}HgN_6Si_8Sn_2$	$C_{56}H_{84}CdN_6Si_8Sn_2$	$C_{56}H_{84}N_6Si_8Sn_2Zn$?½$C_7D_8$
M_r	1503.98	1415.79	1418.85
temperature [K]	140(2)	150(2)	150(2)
wavelength [Å]	0.71073	0.71073	0.71073
crystal system	triclinic	triclinic	triclinic
space group	$P\bar{1}$	$P\bar{1}$	$P\bar{1}$
Z	1	1	2
unit cell dimensions			
a [Å]	10.81440(10)	10.72190(10)	13.97630(10)
b [Å]	12.4358(2)	12.3354(2)	14.05280(10)
c [Å]	13.9143(5)	14.0422(2)	20.3441(2)
α [°]	74.0434(6)	74.7793(6)	96.0161(4)
β [°]	69.2458(6)	69.4183(6)	100.7048(3)
γ [°]	79.8867(6)	80.1274(7)	115.4108(4)
volume [Å^3]	1676.05(4)	1671.22(4)	3468.84(5)
ρ_{calcd} [g cm^{-1}]	1.490 g	1.407	1.358
μ [mm^{-1}]	3.205	1.238	1.235
$F(000)$	754	722	1458
crytal size [mm]	0.30 × 0.30 × 0.30	0.20 × 0.20 × 0.20	0.20 × 0.20 × 0.20
θ range [°]	2.14–26.0	3.98–26.36	3.73 to 25.98
limiting indices	$-13 \le h \le 13$	$-12 \le h \le 13$	$-17 \le h \le 17$
	$-15 \le k \le 15$	$-15 \le k \le 15$	$-17 \le k \le 15$
	$-17 \le l \le 17$	$-17 \le l \le 17$	$-25 \le l \le 24$
reflections collected	23307	27426	45699
independent reflections (R_{int})	6557 (0.0442)	6713 (0.0346)	13229 (0.0392)
refinement method	full-matrix least-squares on F^2	full-matrix least-squares on F^2	full-matrix least-squares on F^2
data/restraints/parameters	6557/0/341	6713/0/341	13229/5/698
$T_{min/max}$	0.38729/0.25607	0.33751/0.30057	0.38284/0.32612
goodness-of-fit on F^2	1.035	1.101	1.069
final R indices R_1	0.0264	0.0244	0.0312
$[I > 2\sigma(I)]$ wR_2	0.0667	0.0572	0.0744
R indices (all data)			
R_1	0.0300	0.0294	0.0385
wR_2	0.0689	0.0599	0.0782
largest diff. peak and hole [e Å^{-3}]	0.963/−1.771	0.551/−0.489	1.078/−1.561

Acknowledgements

We thank the University of Joensuu (Inorganic Materials Chemistry Graduate Program), and the CNRS (France), for funding and Wacker Chemie AG for generous gifts of basic chemicals. We thank Dr. Jean-Pierre Kintzinger for valuable advice and Dr. Pipsa Hirva for technical support (NMR).

[1] For a general discussion of metal–metal bond polarity see: a) L. H. Gade, *Angew. Chem.* **2000**, *112*, 2768; *Angew. Chem. Int. Ed.* **2000**, *37*, 2658; b) G. Jansen, M. Schubart, B. Findeis, L. H. Gade, I. J. Scowen, M. McPartlin, *J. Am. Chem. Soc.* **1998**, *120*, 7239.

[2] D. A. Armitage in *Comprehensive Organometallic Chemistry*, *Vol. 2* (Eds.: G. Wilkinson, F. G. A. Stone, E. W. Abel), Pergamon, New York, **1982**, p. 99.

[3] Examples of Group 12 silyl compounds: a) E. Wiberg, O. Stecher, H.-J. Andrascheck, L. Kreuzbichler, E. Staude, *Angew. Chem.* **1963**, *75*, 516; *Angew. Chem. Int. Ed. Engl.* **1963**, *2*, 507; b) L. Rösch, G. Altmann, *Angew. Chem.* **1979**, *91*, 62; *Angew. Chem. Int. Ed. Engl.* **1979**, *19*, 60; c) L. Rösch, H. Müller, *Angew. Chem.* **1976**, *88*, 681; *Angew. Chem. Int. Ed. Engl.* **1976**, *15*, 620; d) H. Müller, L. Rösch, *J. Organomet. Chem.* **1977**, *133*, 1; e) J. Arnold, T. D. Tilley, A. L. Rheingold, S. J. Geib, *Inorg. Chem.* **1987**, *26*, 2106; f) K. W. Klinkhammer, J. Weidlein, *Z. Anorg. Allg. Chem.* **1996**, *622*, 1209; g) N. Wiberg, K. Amelunxen, H.-W. Lerner, H. Nöth, A. Appel, J. Knizek, K. Polborn, *Z. Anorg. Allg. Chem.* **1997**, *623*, 1861; h) N. Wiberg, W. Niedermayer, H.-W. Lerner, M. Bolte, *Z. Anorg. Allg. Chem.* **2001**, *627*, 1043.

[4] Examples for structurally characterized Ge–Hg bonds: a) L. G. Kuz′mina, T. V. Timofeeva, Yu. T. Struchkov, M. N. Bochkarev, *Zh. Strukt. Khim.* **1981**, *22*, 60; b) K. W. Klinkhammer, *Habilitation Thesis* **1998**, University of Stuttgart; c) S. N. Titova, V. T. Bychkov, G. A. Domrachev, G. A. Razuvaev, L. N. Zakharov, G. G. Aleksandrov, Yu. T. Struchkov, *Inorg. Chim. Acta* **1981**, *50*, 71.

[5] Early examples for Sn–Hg compounds: a) C. Eaborn, A. R.

Thompson, D. R. M. Walton, *Chem. Commun.* **1968**, 1051; b) U. Blaukat, W. P. Neumann, *J. Organomet. Chem.* **1973**, *63*, 27; c) M. F. Larin, D. V. Gendin, V. A. Pestunovich, O. A. Kruglaya, N. S.; Vyazankin, *Izv. Akad. Nauk. SSSR, Ser. Khim.* **1979**, 697.

[6] a) O. A. Kruglaya, G. S. Kalinina, B. I. Petrov, N. S. Vyazankin, *J. Organomet. Chem.* **1972**, *46*, 51; b) G. S. Kalinina, B. I. Petrov, O. A. Kruglaya, N. S. Vyazankin, *Zh. Obshch. Khim.* **1972**, *42*, 148.

[7] a) F. J. A. des Tombe, G. J. M. van der Kerk, H. M. J. C. Creemers, J. G. Noltes, *Chem. Commun.* **1966**, *24*, 914; b) F. J. A. des Tombe, G. J. M. van der Kerk, H. M. J. C. Creemers, N. A. D. Carey, J. G. Noltes, *J. Organomet. Chem.* **1972**, *44*, 247; c) F. J. A. des Tombe, G. J. M. van der Kerk, J. G. Noltes, *J. Organomet. Chem.* **1972**, *43*, 323.

[8] H.-F. Klein, J. Montag, U. Zucha, *Inorg. Chim. Acta* **1990**, *177*, 43.

[9] a) B. Findeis, L. H. Gade, I. J. Scowen, M. McPartlin, *Inorg. Chem.* **1997**, *36*, 960; b) B. Findeis, M. Contel, L. H. Gade, M. Laguna, M. C. Gimeno, I. J. Scowen, M. McPartlin, *Inorg. Chem.* **1997**, *36*, 2386; c) L. H. Gade, *Eur. J. Inorg. Chem.*, **2002**, 1257.

[10] a) K. W. Hellmann, S. Friedrich, L. H. Gade, W.-S. Li, M. McPartlin, *Chem. Ber.* **1995**, *128*, 29; b) M. Contel, K. W. Hellmann, L. H. Gade, I. Scowen, M. McPartlin, M. Laguna, *Inorg. Chem.* **1996**, *35*, 3713; c) K. W. Hellmann, P. Steinert, L. H. Gade, *Inorg. Chem.* **1994**, *33*, 3859; d) K. W. Hellmann, L. H. Gade, O. Gevert, P. Steinert, J. W. Lauher, *Inorg. Chem.* **1995**, *34*, 4069; e) H. Memmler, U. Kauper, L. H. Gade, D. Stalke, J. W. Lauher, *Organometallics* **1996**, *15*, 3637; f) M. Lutz, B. Findeis, M. Haukka, T. A. Pakkanen, L. H. Gade, *Eur. J. Inorg. Chem.* **2001**, 3155.

[11] Holleman-Wiberg, *Lehrbuch der Anorganischen Chemie*, 101 st ed., deGruyter, Berlin **1995**, pp. 1838 – 1841.

[12] a) D. Bravo-Zhivotovskii, M. Yuzefovich, M. Bendikov, K. W. Klinkhammer, Y. Apeloig, *Angew. Chem.* **1999**, *111*, 1169; *Angew. Chem. Int. Ed.* **1999**, *38*, 1100; b) W. H. Ilsley, E. A. Sadurski, T. F. Schaaf, M. J. Albright, T. J. Anderson, M. D. Glick, J. P. Oliver, J. P. *J. Organomet. Chem.* **1980**, *190*, 257.

[13] M. Lutz, B. Findeis, M. Haukka, T. A. Pakkanen, L. H. Gade, *Organometallics*, **2001**, *20*, 2505.

[14] A. Bayler, A. Schier, G. A. Bowmaker, H. Schmidbaur, *J. Am. Chem. Soc.* **1996**, *118*, 7006.

[15] a) I. Dance, M. Scudder, *Chem. Eur. J.* **1996**, *2*, 481; b) C. Hasselgren, P. A. W. Dean, M. L. Scudder, D. C. Craig, I. G. Dance, *J. Chem. Soc. Dalton Trans.* **1997**, 2019; c) M. Scudder, I. Dance, *J. Chem. Soc. Dalton Trans.* **1998**, 329; d) M. Scudder, I. Dance, *J. Chem. Soc. Dalton Trans.* **1998**, 3167; e) G. R. Lewis, I. Dance, *J. Chem. Soc. Dalton Trans.* **2000**, 299; f) I. Dance, M. Scudder, *J. Chem. Soc. Dalton Trans.* **2000**, 1579; M. Scudder, I. Dance, *J. Chem. Soc. Dalton Trans.* **2000**, 2909.

[16] J. T. B. H. Jastrzebski, H. A. J. Sypkens, F. J. A. des Tombe, P. A. van der Schaaf, J. Boersma, G. van Koten, A. L. Spek, A. J. M. Duisenberg, *J. Organomet. Chem.* **1990**, *396*, 25.

[17] B. Wrackmeyer, *Ann. Rep. NMR Spect.* **1985**, *16*, 73; J. Boersma in *Comprehensive Organometallic Chemistry*, *Vol. 2* (Eds.: G. Wilkinson, F. G. A. Stone, E. W. Abel), Pergamon, New York, **1982**, pp. 823.

[18] a) A. Bax, D. G. Davis, *J. Magn. Reson.* **1985**, *63*, 207; b) H. Desvaux, P. Berthault, N.Birlirakis, M. Goldman, M. Piotto, *J. Magn. Reson. A* **1995**, *13*, 47.

[19] a) R. G. Pearson, *J. Am. Chem. Soc.* **1963**, *85*, 3533; b) R. G. Pearson, *Hard and Soft Acids and Bases*, Dowden, Hutchinson and Ross, Stroudsburg, **1973**; c) R. G. Parr, R. G. Pearson, *J. Am. Chem. Soc.* **1983**, *105*, 7512.

[20] *Collect Data Collection Software*, Nonius B. V., 1997 – 2000.

[21] Z. Otwinowski, and W. Minor, W., DENZO-SCALEPACK, "Processing of X-Ray Diffraction Data Collected in Oscillation Mode", in *Methods in Enzymology*, *Volume 276, Macromolecular Crystallography, part A*, (Eds.: C. W. Carter, Jr., R. M. Sweet), Academic Press, New York, **1997**, p. 307.

[22] A. Altomare, M. C. Burla, M. Camalli, G. L. Cascarano, C. Giacovazzo, A. Guagliardi, A. G. Moliterni, G. Polidori, R. J. Spagna, *Appl. Cryst.* **1999**, *32*, 115.

[23] L. J. Farrugia, *J. Appl. Cryst.* **1999**, *32*, 837.

[24] P. T. Beurskens, G. Beurskens, R. de Gelder, S. Garcia-Granda, R. O. Gould, R. Israel, J. M. M. Smits, The DIRDIF-99 program system, Crystallography Laboratory, University of Nijmegen, The Netherlands, **1999**.

[25] G. M. Sheldrick, SHELXTL Version 5.1, Bruker Analytical X-ray Systems, Bruker AXS, Inc.Madison, Wisconsin, USA, **1998**.

[26] G. M. Sheldrick, SHELXL-97, Program for Crystal Structure Refinement, University of Göttingen, Germany, **1997**.

Received: March 7, 2002 [F3932]

  0947-6539/02/0814-3276 $ 20.00+.50/0